

## FERRITE HOM LOAD SURROUNDING A CERAMIC BREAK\*

L. Hammons<sup>#</sup>, Brookhaven National Laboratory, Upton NY 11793 and  
the State University of New York at Stony Brook, Stony Brook, NY 11794

H. Hahn, Brookhaven National Laboratory, Upton, NY 11793

### Abstract

Several future accelerator projects at the Relativistic Heavy Ion Collider are being developed using a superconducting electron energy recovery LINAC along with a superconducting electron gun as the source. All of the projects involve high-current, high-charge operation and require effective higher-order mode (HOM) damping to achieve the performance objectives. Among the HOM designs being developed is a waveguide-type HOM load for the electron gun consisting of a ceramic break surrounded by ferrite tiles. This design is innovative in its approach and achieves a variety of ends including broadband HOM damping and protection of the superconducting cavity from potential damage to the ferrite tiles. Furthermore, the ceramic is an effective thermal transition. This design may be useful in various applications since it readily allows for replacement of the ferrite tiles with other materials and may also be useful for testing the absorbing properties of these materials. In this paper, the details of the design will be discussed along with current modelling and testing results as well as future plans.

### INTRODUCTION

The physics needs and technical requirements for several future accelerator projects at the Relativistic Heavy Ion Collider (RHIC) all involve the use of Energy Recovery LINACs (ERLs). These projects include high-current, high-charge operating parameters that make effective HOM damping essential. They include the development of an experimental 703 MHz energy recovery LINAC [1]; the study of superconducting cavities for a polarized electron-ion collider (eRHIC) [2]; and development of coherent electron cooling [3].

The experimental ERL facility aims to demonstrate operation with an average beam current in the range of 500 mA, combined with very-high-efficiency energy recovery. The facility includes a five-cell superconducting LINAC plus a 1/2-cell superconducting, photoinjector RF electron gun, both operating at 703.75 MHz [4].

This paper discusses the HOM load that is intended for the 1/2-cell superconducting electron gun. The damper shall be placed downstream of the gun and features a novel design that surrounds a ceramic break with microwave-absorbing ferrite material. The inside of the ceramic is coated with a thin film of titanium-stabilized stainless steel to prevent static charge accumulation. The ceramic break protects the vacuum chamber and the superconducting cavity upstream of the damper from the particulates that could arise due to damage of the ferrite tiles. The ceramic allows higher-order modes to penetrate

the dielectric material and interact with the high-permeability ferrite via the magnetic fields of the modes. The ceramic is also an effective thermal transition that may be useful in various applications, and, when coupled with the design of the “clamshell” structure that holds the ferrite in place, allows other damping materials to be rapidly substituted and tested.

To study HOM damping, a series of measurements was conducted on the absorber by itself and attached to the niobium cavity at room temperature. In these studies, the ceramic coating was not taken into account. The coating requires an additional R&D effort to properly apply since the break consists of a ceramic tube to which metallic cuffs have been joined on either side, and it is challenging to ensure electrical continuity from the coating layer to the metal cuffs. To date, efforts at sputter-coating the ceramic and ensuring continuity are being planned, but no coated articles are yet available for measurement. Details of the coating and its surface impedance have been discussed elsewhere [5], [6] including these proceedings [7].

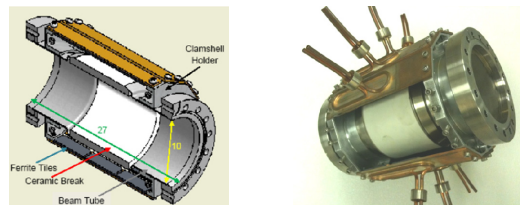


Figure 1: Schematic diagram of ceramic break surrounded by ferrite tiles attached to metal plates with dimensions in cm (left) along with actual HOM load with some plates removed to expose ceramic (right).

### THE FERRITE ABSORBER SURROUNDING A CERAMIC BREAK

The absorber consists of an alumina ceramic break surrounded by ferrite tiles attached to aluminium plates. These plates are arranged in a clamshell-like holder that clamps around the ceramic as shown in Figure 3. The alumina thickness is 1.1 cm and the beampipe inner radius is 5.08 cm. The clamshell holds the ferrite tiles at an inner radius of 7.105 cm from the center of the beampipe. The ferrite tiles are made from C48 ferrite [8] and room-temperature properties were measured by Mouris and Hutcheon [9] for the Canadian Light Source. The two ends of the damper were covered with shorting plates and short probes were inserted in either end for measurement of the  $S_{21}$  parameter using a network analyzer from 1.8 - 3.8 GHz from which  $Q$ -values were determined. These measurements were compared to an identical length of smooth beampipe as a reference, and the two are compared in Figure 2.

\*Work supported by Brookhaven Science Associates, LLC under Contract No. DE-AC02-98CH10886 with the U.S. Department of Energy.  
<sup>#</sup>hammons@bnl.gov

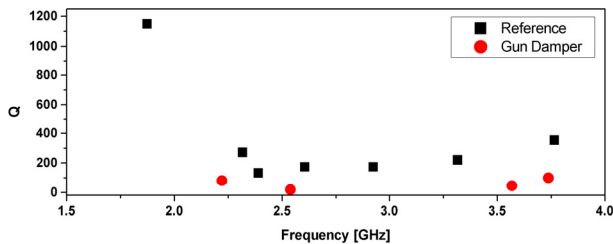


Figure 2: Comparison of  $Q$ -values and resonant frequencies for reference beampipe and ferrite/ceramic damper.

The results show significant damping of HOMs in the ceramic/ferrite structure and significant shifts in frequency and signal coupling, likely attributable to the very different geometries of the reference beampipe and the absorber.

## SIMULATION RESULTS

Simulation studies using CST Microwave Studio [10] were also conducted to determine the damping performance of the HOM absorber connected to the niobium gun cavity. For the first of these studies, the eigenmode solver was used to establish the higher order modes of the cavity and determine the shunt impedances. Shunt impedances were calculated using the data from the simulation model at each resonance. These results are tabulated for selected ( $R/Q > 1$ ) in Table 1 for monopole and dipole modes respectively. The  $Q$ -value was calculated for superconducting niobium at 4K.

Table 1: Selected Monopole and Dipole Modes in the Superconducting Gun

Frequency [GHz]	$Q_{MWS}$	$R/Q$ [ $\Omega$ ]	Mode Type
0.704098	$1.96 \times 10^9$	96.06	Monopole
1.006489	$5.44 \times 10^7$	47.19	Dipole
1.488837	$1.90 \times 10^8$	55.26	Monopole
1.700017	$1.91 \times 10^8$	7.48	Dipole
1.840611	$1.29 \times 10^8$	2.14	Dipole
1.891841	$2.26 \times 10^7$	3.41	Dipole
1.952149	$2.48 \times 10^7$	1.23	Dipole
2.250506	$4.56 \times 10^7$	10.82	Monopole
2.335711	$8.16 \times 10^8$	1.77	Monopole
2.384878	$5.93 \times 10^8$	1.18	Monopole
2.632224	$1.33 \times 10^7$	1.20	Dipole
2.989171	$2.59 \times 10^7$	6.69	Monopole

In subsequent studies, a model (Figure 4) was constructed that included the gun attached directly to the ceramic/ferrite damper, similar to the configuration used for bench measurements. The structure was stimulated using “waveguide” ports (simulating perfect impedance matching with-out reflection at all frequencies) at the fundamental power coupler port and the beampipe end. The  $S_{21}$  transmission coefficient was calculated for two different configurations of the HOM absorber: the full absorber with ceramic and ferrite as well as with the ceramic removed. In addition, the  $S_{21}$  coefficient was also calculated for a reference configuration in which the gun was attached to a straight section of beampipe. The results are compared in Figure 5.

The plot shows that the ceramic/ferrite combination has the lowest signal transmission of all three cases throughout much of the 2 - 3 GHz range. It is interesting that the

coefficients for the ceramic/ferrite absorber and the reference are equivalent at the lowest frequencies up to the dipole doublet resonance at  $\sim 2.2$  GHz. The ferrite alone shows the greatest damping throughout this range up to  $\sim 2.33$  GHz. Beyond this frequency, the ceramic/ferrite combination indicates somewhat greater damping.

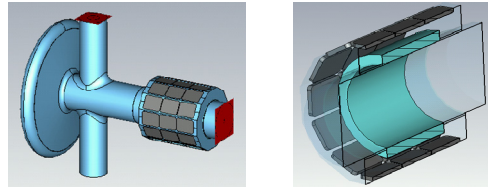


Figure 4: Simulation model (left) of gun cavity with damper and cutaway view of ceramic/ferrite damper (right). Red squares on left show waveguide ports used to stimulate the structure.

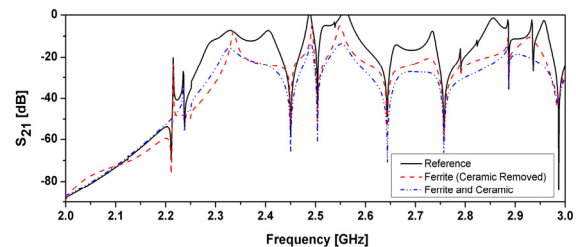


Figure 5: Plot of  $S_{21}$  coefficient from simulation of three cases: straight section of beampipe of equivalent length to ceramic/ferrite absorber (reference), absorber without ceramic, and full ceramic/ferrite absorber.

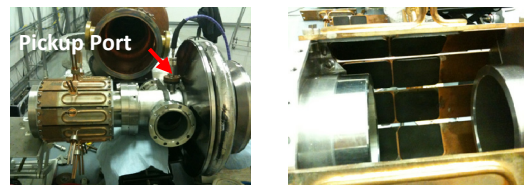


Figure 6: Basic measurement configuration with full HOM load directly attached to gun cavity (left). For measurements, all ports were covered with shorting plates. Also shown (right) is measurement configuration in which ceramic is missing but ferrite is attached. Notice ferrite tiles used in test do not fully cover ceramic.

## MEASUREMENT OF DAMPING IN THE CERAMIC/FERRITE ABSORBER

Finally, room temperature  $S_{21}$  measurements of the ceramic/ferrite absorber were conducted to determine the frequency and  $Q$ -value of damped modes. Various configurations were used for comparison, but all measurements involved attaching some form of the damping structure under test directly to the gun cavity as shown in Figure 7. The structure was then stimulated from the cathode port at the rear of the cavity, and all ports were covered with shorting plates. The pickup port (shown in Figure 7) was used to insert the pickup probe, and  $S_{21}$  transmission measurements were conducted using a network analyzer. Frequency and  $Q$ -values were also obtained using the 3-dB method.

The full structure with both ceramic and ferrite tiles was compared to a structure with only the ferrite tiles and the ceramic removed as well as a structure in which only the ceramic break was used, wrapped in a metallic sheath such that electric continuity along the length of the pipe was ensured. Thereby, the damping of the various components of the HOM absorber could be compared to the full structure. Note that in these measurements, a prototype set of plates with only two ferrite tiles attached to each rather than three was used. Consequently, the ferrite tiles did not fully cover the ceramic absorber in contrast to simulation models. Results from measurements might therefore be expected to show somewhat less damping than if the three ferrite tiles were attached to each plate.

Figure 8 compares the monopole and dipole  $Q$ -values from 0.5 - 3 GHz for a reference structure, in which a smooth section of beampipe equivalent in length to the HOM absorber was used, to the full HOM absorber, both of which were attached to the gun. The results clearly show significant damping for the ceramic/ferrite absorber at frequencies above  $\sim 1.75$  GHz. Below this frequency, HOMs appear to be completely uncoupled to the absorber. This is explained by the cutoff value of the beampipe at about 1.7 GHz for the  $TE_{11}$  mode. Modes below this frequency simply do not reach the HOM absorber, and therefore, are undamped. There is also an undamped dipole mode at 2.15 GHz. However, it has a rather low  $R/Q$  value ( $0.16 \Omega$ ) and is likely of little concern for beam dynamics. All other modes are very effectively damped and many of the resonances that appeared for the reference structure are absent when the full HOM absorber is attached.

Figure 9 shows the  $Q$ -values for the configuration with the ceramic removed as well as the ceramic alone wrapped in a metallic sheath. The results indicate that while the ceramic/ferrite absorber gives the best damping performance for all monopole and dipole modes, ferrite alone without the ceramic provides more effective damping than the ceramic alone suggesting that the ceramic by itself contributes little to the damping. This is expected since alumina is relatively loss-free. Furthermore, the results appear to have been anticipated by the simulation studies. The only exception appears to be the mode at  $\sim 2.25$  GHz where the ceramic shows a lower  $Q$ -value than the ferrite alone. This might be attributed to contact losses that simply predominated in the ceramic case at this frequency or changes in geometry that have not been fully accounted for. Nonetheless, the majority of modes show greater damping by the ferrite.

## CONCLUSIONS

The results show that the combination of a ceramic break surrounded by ferrite is effective for damping the higher-order modes of the gun cavity. The advantages of this novel design include its simplicity and the protection it provides against dust or chips that might result from damage to the ferrite tiles that serve as the HOM absorbing material. The ceramic is also an effective thermal transition that may be useful in various applications. Fur-

thermore, the use of the ceramic break, coupled with the design of the “clamshell” structure that holds the ferrite tiles in place, allows other damping materials to be quickly and easily substituted. The results included simulations and measurements of the damper attached to the gun cavity, all of which confirm that the performance of the damper lowers the  $Q$ -value of higher-order modes significantly. Furthermore, all of the results suggest that the presence of the ceramic layer appears to enhance the damping of certain modes. However, the ceramic must be coated to prevent static charge accumulation, and this is likely to affect the damping performance. This will require additional R&D activity, and measurements of damping with a coated ceramic remain to be performed.

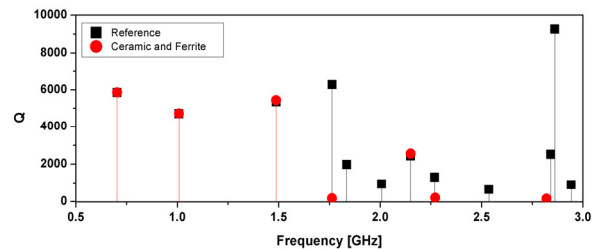


Figure 8: Plot of monopole and dipole  $Q$ -values for cavity attached to smooth beampipe (reference) and ceramic/ferrite HOM absorber.

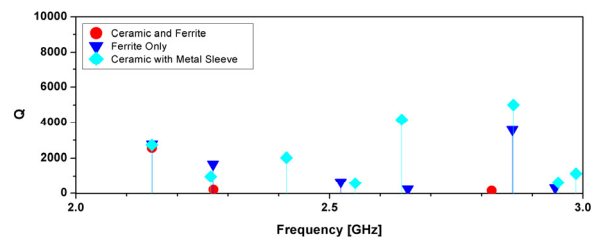


Figure 9: Monopole and dipole  $Q$ -values for full HOM absorber, absorber with ferrite alone (no ceramic), and with ceramic alone (no ferrite).

## ACKNOWLEDGEMENTS

The authors are grateful to Dr. V. Litvinenko and Dr. I. Ben-Zvi for their vision of the project, many fruitful discussions, and their helpful advice.

## REFERENCES

- [1] V. N. Litvinenko, et al., 2007 IEEE Particle Accelerator Conference, 1347 (2007).
- [2] V. Ptitsyn, et al., in EPAC 2004, Switzerland (2004).
- [3] V. N. Litvinenko and Y. S. Derbenev, Physical Review Letters 102 (2009).
- [4] R. Calaga, et al., Physica C - Superconductivity and Its Applications 441, 159 (2006).
- [5] H. Hahn, Report C-A/AP/#336, Brookhaven National Laboratory, Upton, NY (2008).
- [6] H. Hahn, Physical Review Special Topics-Accelerators and Beams, 012002 (2010).
- [7] H. Hahn and L. Hammons, these proceedings.
- [8] Countis Laboratories, Grass Valley, CA 95945.
- [9] J. Mouris and R. Hutcheon, Microwave Properties North, Ontario, Canada (2000).
- [10] Computer Simulation Technology AG (2008).